Isolation System with Wireless Power Transfer for Multiple Gate Driver Supplies of a Medium Voltage Inverter

Keisuke Kusaka, Koji Orikawa and Jun-ichi Itoh
Dept. of Energy and Environmental
Nagaoka University of Technology
Nagaoka, Niigata, Japan
kusaka@stn.nagaokaut.ac.jp

Kazunori Morita and Kuniaki Hirao
Research & Development Group
Meidensha Corporation
Numazu, Japan

***Abstract*— In this paper, a multiple wireless power transfer system for multiple gate driver supplies of a medium voltage inverter is developed. The proposed isolation system achieves a galvanic isolation with an air-gap of 50 mm using a wireless power transfer with magnetic resonance coupling. It easily respects the standard of galvanic isolation, which is established by International electrotechnical commission (IEC). Moreover, the power is supplied from one transmitting board to six gate drivers without a solid magnetic core. In this paper, the isolation system is developed and tested. It is clarified that the isolation system transmits power of not less than 300 mW to each gate drivers beyond an air-gap. However, sum of the output power of the each receiving board are limited up to approximately 3.5 W because of a voltage drop in the equivalent series resistances of the transmission coils.**

Keywords*— *Galvanic isolation, Medium voltage inverter, Wireless power transfer, Magnetic Resonance Coupling

I. Introduction

In recent years, system voltage of a three-phase medium voltage inverter for a motor drive system is rising to 3.3 kV and 6.6 kV. In the medium voltage inverter, galvanic isolations are required at gate driver supplies. The safety standards, which are established by IEC [1], have to be satisfied for safety. The safety standards require a minimum clearance of 14 mm and a creepage distance of 81 mm when a system voltage of the inverter is 6.6 kV, a comparative tracking index (CTI) is $100 \leq \text{CTI} < 400$ and a pollution degree is two [1].

In general, isolation transformers with solid magnetic cores are used for a galvanic isolation. However, it causes an increase in a cost because it is typically custom-built. Moreover, the isolation transformer is huge in order to obtain a high isolation voltage. For example, a typical dimension of the isolation transformer, which have an isolation voltage of 20 kV_{rms} for 10 s, are 200 mm × 200 mm × 200 mm at a weight of approximately 5.5 kg [2]. These transformers are placed at each gate driver supplies.

In order to achieve a cost reduction and a downsizing of the isolation system, a single-chip DC-isolated gate drive IC has been demonstrated [3-5]. It supplies power using a microwave from a bottom layer of a sapphire substrate to a top layer. In this method, galvanic isolation is achieved by the sapphire substrate. It can downsize an isolation system vastly. However, it does not satisfy the safety standards because both of an isolation distance and a creepage distance are not enough.

Meanwhile, J. W. Kolar et al. proposed the isolation system with using a printed circuit board (PCB) [6]. It achieves a galvanic isolation with a coreless transformer. In this system, one transmitting side transmits power to a receiving side one-by-one (1×1). Thus, the systems are also required at each gate driver supply. Therefore the reduction of the volume is limited.

In this paper, a galvanic isolation system with a multiple wireless power transfer system with magnetic resonance coupling for a medium voltage inverter is developed. The isolation system transmits power from one transmitting board to six receiving boards (1×6) beyond an air-gap of 50 mm. Because all of the isolation system is constructed by the PCBs. The isolation system contributes a cost reduction and a downsizing of the isolation system. Besides, the insulation with an air-gap of 50 mm easily respects IEC standard of a clearance and a creepage distance, when the system voltage of the inverter is 6.6 kV. Moreover, the air-gap of 50 mm reduces a common-mode current, which is induced by high *dv*/*dt* of the medium voltage inverter, to a small-signal circuit.

II. Proposed Isolation System

A. System Configuration

Fig. 1 shows the system configuration of the developed galvanic isolation system for a medium voltage inverter. The isolation system consists of the transmitting board and six receiving boards. The power consumption in the gate drive units (GDUs) is supplied through the isolation system from the low-voltage power supply of 48 V in a medium voltage inverter.

Incidentally, magnetic resonance coupling achieves a wireless power transfer with a resonance with a high-quality factor Q of the transmission coils in a middle-range transmission distance [7-12]. In this system, 2.18 MHz is used as the transmission frequency because a high-frequency transmission is required in order to downsize the transmission coils. Then the isolation system does not require a transformer with a magnetic core. In the conventional system, the transformer with a magnetic core prevents an isolation system from a cost reduction and a downsizing. In contrast, the isolation system is constructed only by the PCBs in this system. The PCBs can be manufactured easily in comparison with the transformer.

Fig. 2 shows the positional relationship of the transmitting board and the receiving boards. The maximum size of the system is constrained up to 300 mm × 150 mm × 150 mm for a reason of the space limitations of the medium voltage inverter. The receiving boards are placed at top and bottom of the transmitting board. Each distance between the receiving boards and the transmitting board is kept at not less than 50 mm for the galvanic isolation. It contributes the high isolation voltage and a low common-mode current through leakage capacitances. It is enough to fulfill the safety standards of IEC [1] when the operating voltage of the medium voltage inverter is 6.6 kV.

The transmitting boards consist of a high-frequency inverter, a series resonance capacitor and a transmitting coil for a wireless power transfer system. The inverter is operated by a square-wave operation with an output frequency of 2.18 MHz because high-frequency operation is necessary in order to downsize the transmission coils on the PCB. On the other hand, the receiving boards consist of a receiving coil, series resonance capacitor and a diode bridge rectifier.

Fig. 3 shows the photograph of the prototype of the isolation system. Each board is placed according to the Fig. 2. Table I indicates the specifications of transmitting coil and receiving coils.

B. *Rated Power of Gate Driver Supplies*

The isolation system transmits the power consumption of the gate drivers. In this subsection, required power of the each gate driver is calculated.

Fig. 4 shows the five-level diode-clamped multilevel inverter as a medium voltage inverter, which has a rated output voltage of 6.6 kV and a rated output power of 1 MVA [13]. Each switching device is a string of three 1.7-kV IGBTs connected in series. The power consumption of a gate resistance P_G of an IGBT is calculated by (1) where f_c is a switching frequency, Q_g is total gate charge and V_{GE} are gate-emitter voltage of the IGBT.

$$P_G = f_c\left(\left|+Q_g\right| + \left|-Q_g\right|\right)\left(\left|+V_{GE}\right| + \left|-V_{GE}\right|\right) \tag{1}$$

From eq. (1), the power consumption is calculated as about 60 mW where a switching frequency of the medium voltage inverter is 1 kHz, total gate charges $\pm Q_g$ are ±1000 nC and gate-emitter voltage is ±15 V. Note that the values, which is used in this calculation, are typical value of an IGBT (V_{CE} = 1700V, I_C = 150 A). Considering a power loss in a gate driver circuit, power of at least 120 mW is required per one receiving board as the output power of the isolation system.

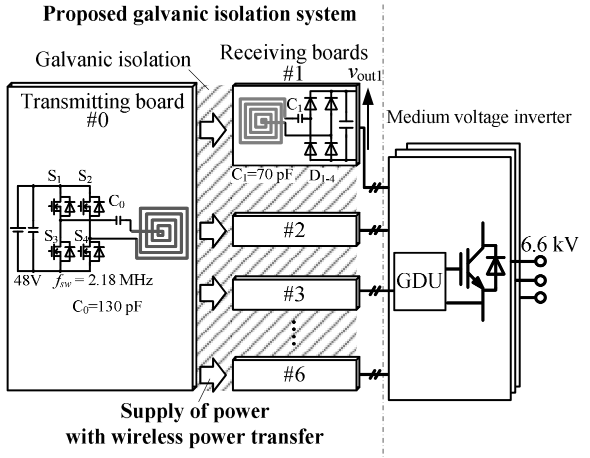

Fig. 1. System configuration of the developed isolation system. Power is transmitted from the transmitting board to the six receiving boards by a wireless power transfer with magnetic resonance coupling.

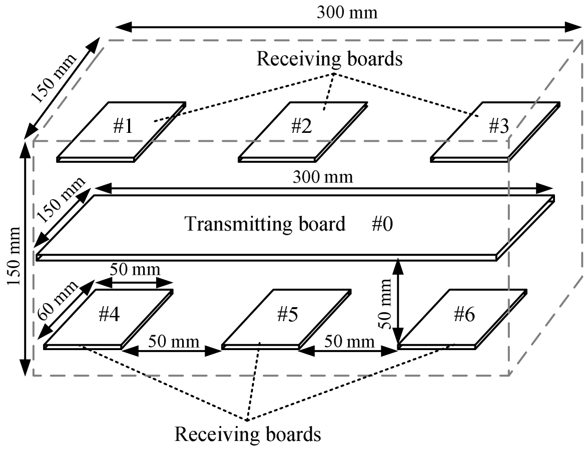

Fig. 2. Placements of each boards of the proposed isolation system. The receiving boards are placed up and down to the transmitting board. Each board are placed keeping an air-gap of 50 mm.

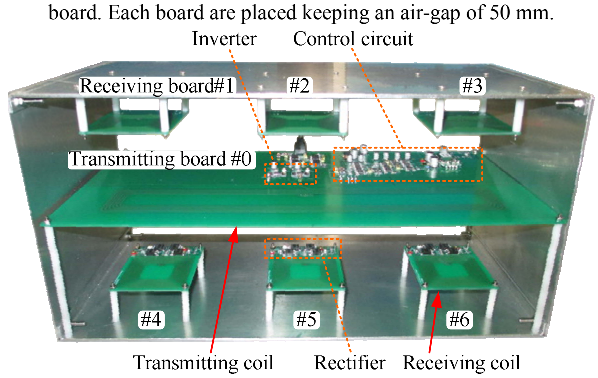

Fig. 3. Photograph of proposed isolation system.

III. Frequency Characteristics with Electromagnetic Analysis

In this section, the part of the wireless power transfer in the isolation system is analyzed with the electromagnetic analysis with Agilent advanced design system (ADS). In ADS, a 3-D model is analyzed by the momentum method.

Table I shows the specifications of the coils for the analysis. The isolation system transmits power with the wireless power transfer with the series resonance capacitors. The windings of the coils are made up on the surfaces of the PCBs. In the system, series resonance capacitor in the transmitting side and series resonance capacitors in the receiving side, which is called as S/S resonance, are used. The resonance capacitors on the transmitting board and the receiving boards are 130 pF and 70 pF, respectively. The wireless power transfer with S/S resonance type has an advantage compared to other method such as a series resonance and parallel resonance (S/P), parallel resonance and parallel resonances (P/P) from the standpoint of the variation of a coupling coefficient and a load. The load characteristics do not affect the resonance frequency in S/S resonance. It is suitable characteristic for the isolation system because the loads have different value in each GDU in the isolation system. Also, the coupling coefficient does not affect the resonance frequency in the S/S resonance. The coupling coefficients vary among the receiving boards. It means that, the isolation system with S/S resonance can be operated at a constant operating frequency without a complex control.

Fig. 5 presents the definition of S-parameters. The S-parameter is one of the methods to express the characteristics of a multi-terminal circuit. The relationship between a square root of input power and a square root of output power is expressed by the matrix shown as eq. (2) where a_1 is a square root of travelling power, b_1 is a square root of reflected power in the primary side, a_2 is a square root of travelling power and b_2 is a square root of reflected power in the secondary side. In this paper, the S-parameters are used to analyze the characteristics of the isolation system.

$$\begin{pmatrix} a_1 \\ b_1 \end{pmatrix} = \begin{pmatrix} S(1,1) & S(1,2) \\ S(2,1) & S(2,2) \end{pmatrix} \begin{pmatrix} a_2 \\ b_2 \end{pmatrix} \tag{2}$$

Fig. 6 shows the definition of S-parameters in the system. In this consideration, a S-parameter S(n,0) is especially focused. The S-parameter S(n,0) is the ratio of a square root of power from the transmitting board to the receiving boards, where n is the number of the receiving boards ($n = 1, 2, \cdots, 6$). In the isolation system, the power flow is limited to one-way; from the transmitting board to the receiving board. Thus, the transmission from the receiving boards (#n) to the transmitting board (#0) can be ignored.

Fig. 7 shows the S-parameters S(n,0) of the system. The S-parameters S(2,0) and S(5,0) reach to -9 dB at the resonance frequency. It means that the each ratio of the output power of

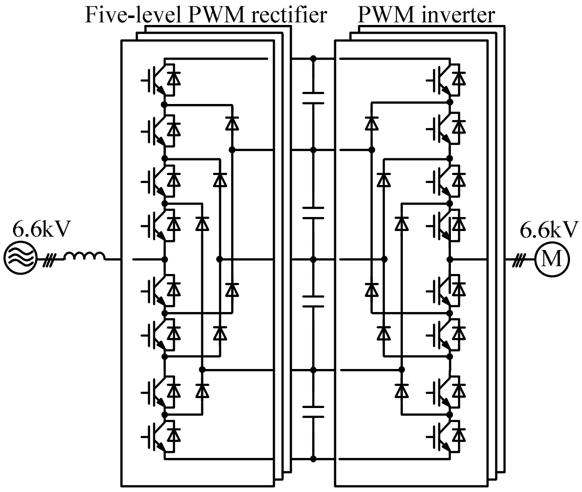

Fig. 4. Assumed 6.6 kV, 1 MVA five-level diode-clamped medium voltage invertere.

Table I. Specification of coils.

(a) Transmitting coil.

Items	Values		Remarks
Number of turn	12	turn	Short type
Width	250	mm	
Depth	40	mm	
Line width	1	mm	
Gap between windings	0.7	mm	
Thickness of PCB	1.6	mm	FR-4
Film thickness of copper	70	µm	

(b) Receiving coils.

Items	Values		Remarks
Number of turns	40	turn	Short type
Outer diameter	44	mm	
Inner diameter	22	mm	
Gap between windings	0.4	mm	
Line width	0.2	mm	
Thickness of PCB	1.6	mm	FR-4

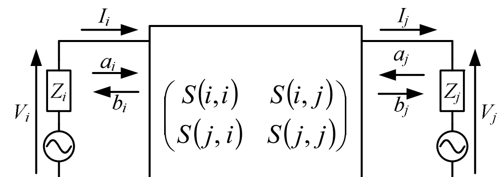

Fig. 5. Definition of S-parameters.

the receiving boards (#2 and #5) to input power of the transmitting board are 13.2%. In contrast, the S-parameters S(1,0), S(3,0), S(4,0) and S(6,0) cannot reach to -10 dB. Thus, the each ratio of the output power of the receiving boards (#1, #3, #4 and #6) to input power calculated as 7.4 %. The non-uniform transmitted power is caused by the difference in the coupling coefficient among the boards. The receiving boards, which are placed in center (#2 and #5) are coupled to the transmitting board (#0) strongly compared to other boards.

Fig. 8 shows the effect between the abutting receiving

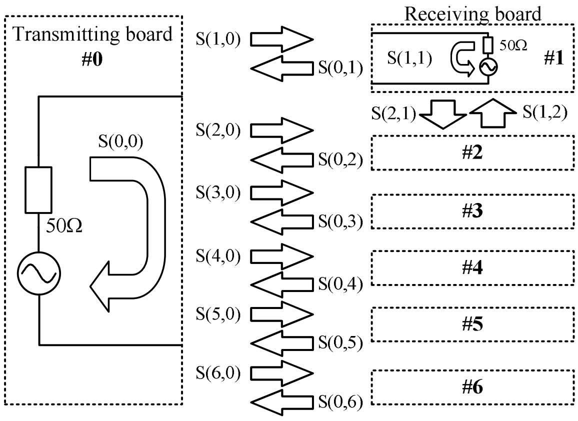

Fig. 6. S-parameters in the isolation system. All of the boards are numbered from #0 to #6. All of the analyses with S-parameters in this paper are held with a characteristic impedance of 50 Ω.

boards. The transmission between the receiving boards is significantly small than the transmission between the transmitting board (#0) and the receiving boards (#1-6). For example, the transmission from the transmitting board (#0) to the receiving board (#1) S(1,0) reaches to -11.4 dB. On the other hand, the transmission from the receiving board (#2) to the receiving board (#1) S(1,2) is a -17.3 dB. Thus, the coupling between the receiving boards can be ignored in the system.

Fig. 9 shows the simulated transmission efficiency. The simulation is held without the converters such as an inverter and a rectifier. The transmission efficiency expresses the ratio of sum of the received power on the receiving boards to the transmitted power from the transmitting board. Thus, the transmission efficiency η_T is calculated by (3). It should be noted that the output impedance of the power supply and the load impedance, which are used for an analysis, are 50 Ω.

$$\eta_T = \sum_{n=1,2,\cdots 6} S(n,0)^2 \tag{3}$$

At a resonance frequency of 2.18 MHz, the total transmission efficiency increases drastically because magnetic resonance coupling achieves the efficient wireless power transfer with a high quality factor Q. The maximum transmission efficiency reaches to 53.6% at 2.18 MHz.

In the isolation system, low transmission efficiency is accepted because the power loss in the proposed isolation system is extremely low compared to the power loss of a medium voltage inverter, typically. Thus, the power loss of the isolation system can be ignored.

IV. TIME-DOMAIN ANALYSIS

A. Equivalent Circuit

Fig. 10 presents the equivalent circuit of the wireless power transfer [14-15] where $r_{0\text{-}6}$ are the equivalent series resistances of the windings and $C_{0\text{-}6}$ are the series resonance capacitors. The equivalent circuit of the multiple wireless power transfer

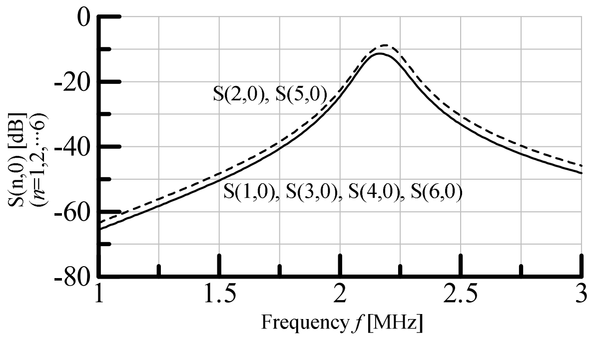

Fig. 7. Positional dependence of the receiving boards on the S-parameters. The S-parameters between the transmitting board #0 and the receiving board #2, 5 are larger than the S-parameter between the receiving board #0 and #1, 3, 4, 6.

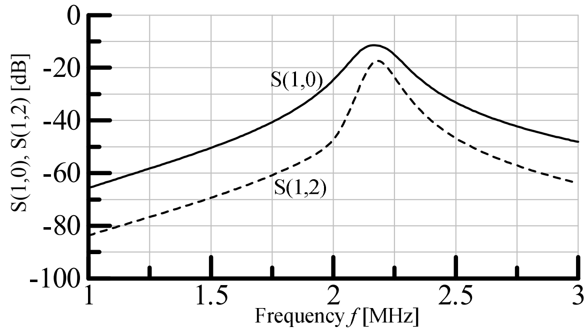

Fig. 8. Effect between the abutting receiving board. The transmission between the receiving boards such as S(1,2) is smaller than the transmission from #0 to #1.

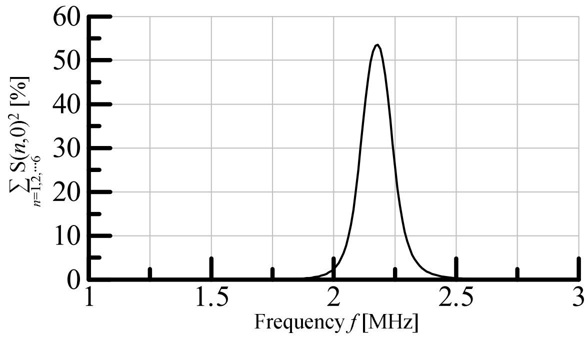

Fig. 9. Transmission efficiency of the isolation system. The efficiency is analyzed from the 3-D model with ADS.

is obtained as transformers with multiple windings where $\boldsymbol{k}$ is the coupling coefficient among the each winding, which is expressed as (4). Note that, the subscript indicates the number of the transmitting board.

$$\mathbf{k} = \begin{pmatrix} 0 & k_{01} & k_{02} & \cdots & k_{06} \\ k_{10} & 0 & k_{12} & \cdots & k_{16} \\ k_{20} & k_{21} & 0 & \cdots & k_{26} \\ \vdots & \vdots & \vdots & \ddots & \vdots \\ k_{60} & k_{61} & k_{62} & \cdots & 0 \end{pmatrix} \tag{4}$$

If the self-inductance of the each winding $\boldsymbol{L}$ is expressed as (5), the leakage inductance $\boldsymbol{L_{le}}$ and magnetizing inductance $\boldsymbol{L_m}$

are provided as (6) and (7), respectively. It should be noted that, k_{ij} is equals to k_{ji} ($i, j = 0, 1, \cdots, 6$).

$$\mathbf{L} = \begin{pmatrix} L_0 & L_1 & L_2 & L_3 & L_4 & L_5 & L_6 \end{pmatrix} \tag{5}$$

$$\mathbf{L}_{\mathbf{le}} = \mathbf{L} - L_0 \begin{pmatrix} 1 & 1 & 1 & 1 & 1 & 1 & 1 \end{pmatrix} \mathbf{k} \tag{6}$$

$$\mathbf{L}_m = \mathbf{L}\mathbf{k} \tag{7}$$

The parameters; the self-inductance, the series resonance capacitors and the coupling coefficients are introduced by the analysis results with ADS at the resonance frequency of 2.18 MHz. Table II shows the derived parameters. In Fig. 10, the coupling coefficients among the receiving boards are ignored because the effect of these coupling is significantly small. It means that the receiving boards are only magnetically coupled to the transmitting board.

Fig. 11 shows the comparison results of the frequency characteristics of the F-parameters. The F-parameters are compared between the equivalent circuit and the 3-D model with ADS in frequency characteristics. ADS indicates the circuit characteristic as S-parameters, typically. Thus, the analysis results are converted to the F-parameters according to eq. (8).

$$\begin{pmatrix} \dot{V}_i \\ \dot{I}_i \end{pmatrix} = \begin{pmatrix} A & B \\ C & D \end{pmatrix} \begin{pmatrix} \dot{V}_j \\ \dot{I}_j \end{pmatrix} = \frac{1}{2S_{ji}} \begin{pmatrix} (1+S_{ii})(1-S_{jj})+S_{ji}S_{ij} & \{(1+S_{ii})(1+S_{jj})-S_{ji}S_{ij}\}\dot{Z}_j \\ \{(1-S_{ii})(1-S_{jj})-S_{ji}S_{ij}\}\dfrac{1}{\dot{Z}_i} & \{(1-S_{ii})(1+S_{jj})+S_{ji}S_{ij}\}\dfrac{\dot{Z}_j}{\dot{Z}_i} \end{pmatrix} \tag{8}$$

The equivalent circuit model shows the good agreement with the 3-D model. The error is caused by the unconsidered parameters; parasitic capacitances between the layers of the PCB, parasitic capacitances between the windings and a dielectric loss of the PCB. These parameters cannot be derived even by the simulation. Furthermore, the error occur owing to the non-linearly characteristics of an impedance of the transmission coils because the impedance of the coils are not proportional to a frequency in the high-frequency region. However, the difference does not cause a fatal error on the time-domain analysis. Thus, the operation model is discussed using the equivalent circuit model in the next subsection.

B. Operation modes

Fig. 12 shows the equivalent circuit with converters for the analysis of the operation modes of the system. The series resonance capacitors are designed according to eq. (9) where ω_{sw} is $2\pi f_{sw}$. The resonance capacitance C_0 on the transmitting board is selected in order to obtain a resonance with the self-inductance of the transmitting coil. Similarly, the resonance capacitances on the receiving boards are selected to resonate with the each self-inductance $\boldsymbol{L}$ of the receiving boards.

$$\mathbf{C} = \frac{1}{\omega_{sw}^2 \mathbf{L}} \tag{9}$$

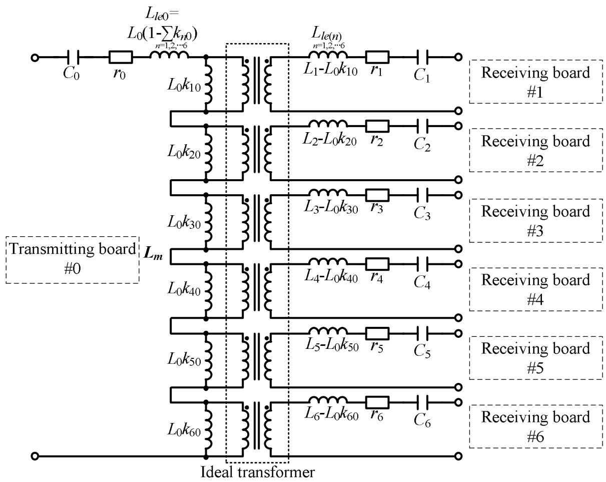

Fig. 10. Simplified equivalent circuit of the proposed isolation system.

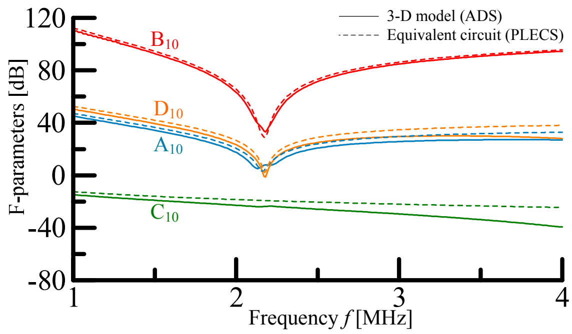

Fig. 11. Comparison results of frequency characteristics between the 3-D model with ADS and the equivalent circuit mode.

Table II. Derived parameter value from the 3-D analysis.

Items		Symbol	Values	
Equivalent series resistances (ESRs)	Board #0	r_0	12.9	Ω
	Board #1	r_1	11.7	Ω
	Board #2	r_2	11.6	Ω
	Board #3	r_3	11.7	Ω
	Board #4	r_4	11.7	Ω
	Board #5	r_5	11.6	Ω
	Board #6	r_6	11.7	Ω
Self-inductances	Board #0	L_0	41.8	μH
	Board #1	L_1	76.5	μH
	Board #2	L_2	75.9	μH
	Board #3	L_3	76.5	μH
	Board #4	L_4	76.5	μH
	Board #5	L_5	75.9	μH
	Board #6	L_6	76.5	μH
Coupling coefficients		k_{01}	0.016	
		k_{02}	0.026	
		k_{03}	0.025	
		k_{04}	0.016	
		k_{05}	0.026	
		k_{06}	0.025	

Fig. 13 shows the vector diagrams of the isolation system. Owing to the resonance based on eq. (9), the inverter voltage and the current are in phase. The terminal voltage of the resonance capacitor and the inductance, become extremely high with opposite directions. Focusing on the receiving side, the resonance capacitor C_1 and the leakage inductance L_{le1} resonate.

Fig. 14 illustrates the simplified operation waveforms of the isolation system.

1) Mode I

The inverter current i_{inv} starts to flow through the MOSFETs and the coils because the MOSFETs S_1 and S_4 are turn-on. Owing to the resonance, the input current becomes a sinusoidal and it is in phase to the inverter output voltage v_{inv} during a period.

2) Mode II

The inverter current i_{inv} commutates to the diodes D_2 and D_4 because the all of MOSFETs turn-off during the dead-time T_d. If the dead-time is significantly short compared to the switching period, the MOSFETs achieve a zero current turn-off owing to the current resonance. After the half of the switching period, the inverter current crosses zero and commutate to the diodes D_1 and D_3. The inverter output voltage is decided by the polarity of the inverter output current.

3) Mode III

The MOSFETs S_2 and S_4 turn-on. The inverter current commutates to the MOSFETs S_2 and S_4 from the diodes. Also, the inverter current is sinusoidal owing to the resonances.

4) Mode IV

The MOSFETs S_2 and S_4 have turned-off at the start of this mode. Owing to the current resonance, the MOSFETs turn-off around a zero current. It contributes a reduction of the switching loss. The inverter currents commutate to the diodes D_1 and D_4. The directions of the inverter current change to a positive from a negative.

V. EXPERIMENTAL RESULTS

A. Fundamental Verifications

Fig. 15 shows the operation waveforms with the prototype, which is shown in Fig. 3. Fig. 15 (a) is the waveforms with no-load condition. Fig. 15 (b) is the loaded waveforms with a resistance load of 107 Ω where the input power of the isolation system is 31.3 W. In this experiment, resistances are used instead of the gate drivers for simplicity.

From the experimental waveforms, it is demonstrated that the wireless power transfer with an air-gap of 50 mm is achieved. An air-gap of 50 mm behaves as an isolation distance. Therefore, it is clear that the isolation system satisfies the safety standards, which is established by IEC [1], when a system voltage of the medium voltage inverter is 6.6 kV.

When the load is not connected, the rectifier input voltage v_{in1} is a sinusoidal because the diodes in the receiving boards do not turn-on. In contrast, the rectifier input voltage becomes

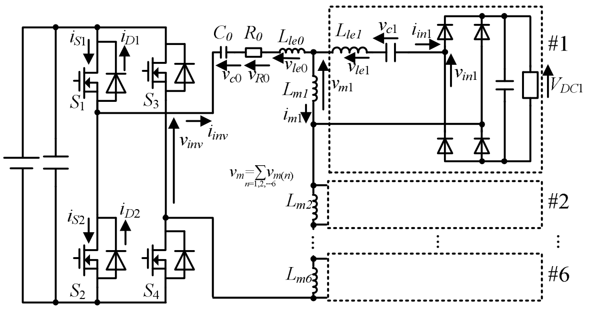

Fig. 12. Equivalent circuit with converters. The ideal transformers are omitted for simplicity.

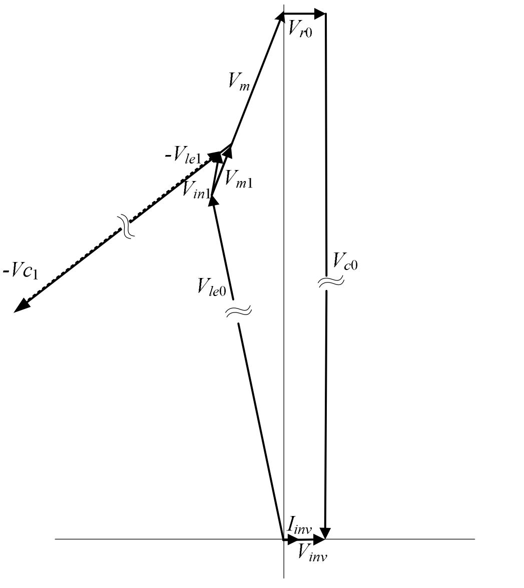

Fig. 13. Vector diagram of the wireless power transfer. The series resonance capacitor C_0 resonates with the sum of leakage inductance L_{le0} and the magnetizing inductance L_m. The self-inductance L_2 and the series resonance capacitor C_1 resonate.

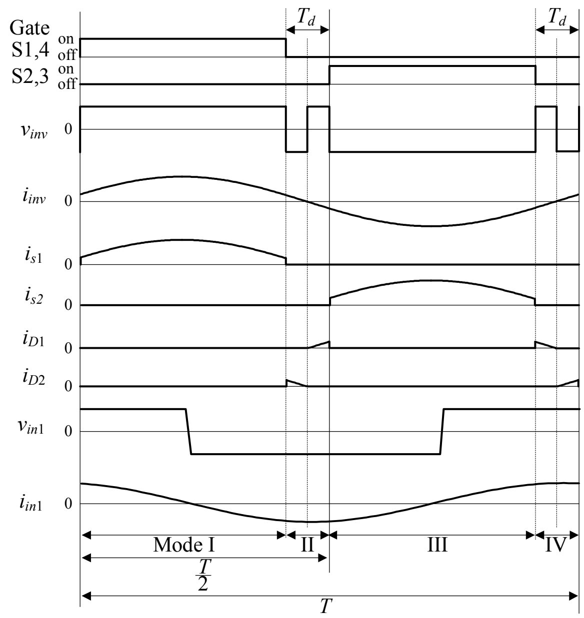

Fig. 14. Simplified operation waveforms. The MOSFETs achieve a zero-current turn-off because of the current resonance.

a trapezoidal wave when the load is connected. This is caused by the sinusoidal-rectifier input current i_{in1}.

As an output voltage, a DC voltage V_{DC1} is obtained despite a load value. However, the output voltage decreases when the load is connected. It is caused by the voltage drop on the equivalent series resistances of the transmission coils $r_{0\text{-}6}$. Incidentally, the others receiving boards simultaneously output the DC voltage. In this paper, the waveforms are omitted due to the page limitations.

Fig. 16 shows the output power of each receiving board. The output power varies among the position of the receiving boards. The difference between the output power is caused by the accuracy of the chassis and differences of the coupling coefficients. In the experimental setup, the output power of the receiving boards (#1, 2, 3) are smaller than that of (#4, 5, 6), respectively because the difference in the transmission distance occur between the upper boards and lower boards. Furthermore, the output power of the receiving boards #2 and #5 are larger than that of adjacent boards, respectively. Thus, the output power of #5 has maximum output power. The minimum output power reaches to 320 mW. It is confirmed that the isolation system supplies the power, which is required in the gate driver supplies.

Fig. 17 shows the total output power P_{out_total} characteristics. The total output power is calculated as (10).

$$P_{out\_total} = \sum_{n=1,2,\cdots,6} P_{out}(n) \tag{10}$$

The output power increases as a load resistance decreases in the interval of the load resistance from 125 Ω to 750 Ω. However, the output power stops to increase when the small resistance such as 107 Ω is connected because the voltage drop on the equivalent series resistances of the transmission coils increases owing to the increment of load current.

B. Operation with Gate Drivers

In this subsection, the prototype with the gate drivers is tested. The gate drivers, which are operated at a switching frequency of 1 kHz, a gate-emitter voltage of ±15V, are connected as a load. Note that DC/DC converters as voltage regulators are connected at the front end of the gate drivers. The DC/DC converter output voltages of ±15 V. Moreover, the photocouplers (Toshiba, TLP250) are used in order to drive the IGBTs in spite of the deficient isolation distance because an isolation of the PWM signal is not a main topic of this paper.

Fig. 18 shows the operation waveforms where the capacitors of 33 nF is connected instead of the IGBTs. Even if the gate drivers are connected as a load, the operation system achieves the wireless power transfer beyond an air-gap of 50 mm.

From the experimental results, it is confirmed that the proposed isolation system can be used as an isolation system for the medium voltage inverter.

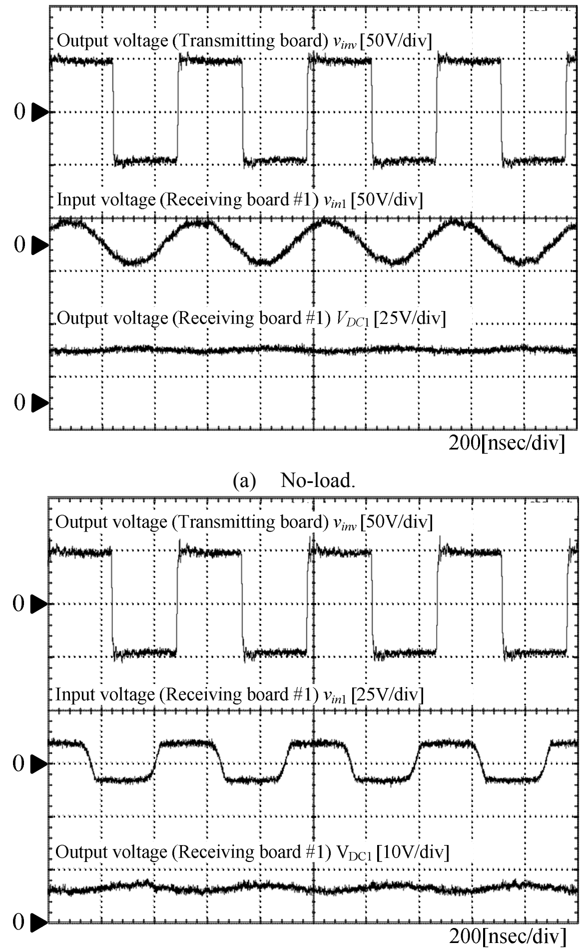

(a) No-load.

(b) Loaded.

Fig. 15. Operation waveforms. The load resistance of 107 Ω is connected as a load instead of a gate driver supplies.

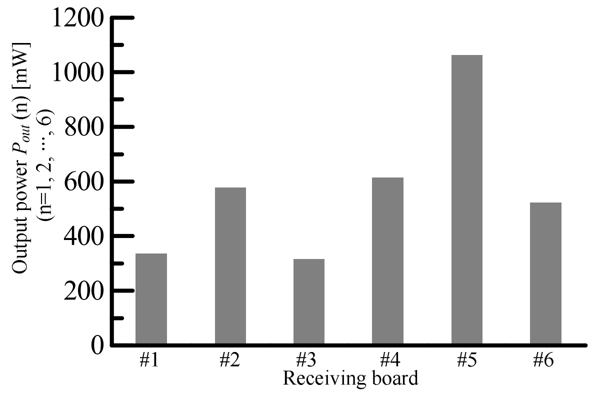

Fig. 16. Operation waveforms. The output power varies among the position of receiving boards. The difference of output power is caused by the difference in the accuracy of the chassis.

VI. CONCLUSIONS

In this paper, the isolation system for gate drivers of a medium voltage inverter with the system voltage of 6.6 kV is reported. The isolation system transmits the power to the six gate drivers beyond the air-gap of 50 mm. The isolation distance satisfies the safety standards in IEC [1]. The isolation system consists of the only seven PCBs. It contributes a cost and weight reduction because it does not need a magnetic core. The experimental results demonstrate that the isolation system supplies the power of not less than 320 mW to the each receiving boards. It is enough power to drive the IGBT in the medium voltage inverter.

REFERENCES

[1] International Electrotechnical Commission (IEC): "Adjustable speed electrical power drive systems – Part 5-1: safety requirements – Electrical, thermal and energy", *IEC 61800-5-1* (2007)

[2] Christoph Marxgut, jurgen Biela, Johann W. Kolar, Reto Steiner, Peter K. Steimer: "DC-DC Converter for Gate Power Supplies with an Optimal Air Transformer", *Applied Power Electronics Conference and Exposition 2010*, pp. 1865-1870 (2010)

[3] S. Nagai, N. Negoro, T. Fukuda, N. Otsuka, H. Sakai, T. Ueda, et al.: "A DC-isolated gate drive IC with drive-by-microwave technology for power switching devices", *International Solid-State Circuits Conference* 2012, pp. 404-406 (2012)

[4] S. Nagai, T. Fukuda, N. Otsuka, D. Ueda, N. Negoro, H. Sakai, et al.: "A one-chip isolated gate driver with an electromagnetic resonant coupler using a SPDT switch", *24th IEEE International Symposium on Power Semiconductor Devices and ICs 2012*, pp. 73-76 (2012)

[5] S. Nagai, N. Negoro, T. Fukuda, H. Sakai, T. Ueda, T. Tanaka, et al.: "Drive-by-Microwave technologies for isolated direct gate drivers", *IEEE Microwave Workshop Series on Innovative Wireless Power Transmission*: Technologies, Systems, and Applications 2012, Vol. , No. , pp. 267-270 (2012)

[6] R. Steiner, P. K. Steimer, F. Krismer, J. W. Kolar: "Contactless Energy transmission for an Isolated 100W Gate Driver Supply of a Medium Voltage Converter", *35th Annual Conference of the IEEE Industrial Electronics Society*, pp. 302-307 (2009)

[7] S. Lee, R. D. Lorenz: "Development and Validation of Model for 95%-Efficiency 200-W Wireless Power Transfer Over a 30-cm Air-gap", *IEEE Trans. On Industry Applications*, Vol. 47, No. 6, pp. 2495-2504 (2011)

[8] T. Imura, Y. Hori: "Maximizing Air Gap and Efficiency of Magnetic Resonant Coupling for Wireless Power Transfer Using Equivalent Circuit and Neumann Formula", *IEEE Trans. On Industrial Electronics*, Vol. 58, No. 10, pp. 4746-4752 (2011)

[9] E. Waffenschmidt, T. Staring: "Limitation of inductive power transfer for consumer applications", *European Conference on Power Electronics and Applications*, pp. 1-10 (2009)

[10] S. Cheon, Y. Kim, S. Kang, M. L. Lee, J. Lee, T. Zyung: "Circuit-Model-Based Analysis of a Wireless Energy-Transfer System via Coupled Magnetic Resonances", *IEEE Trans. On Industrial Electronics*, Vol. 58, No. 7, pp. 2906-2914 (2011)

[11] A. P. Sample, D. A. Meyer, J. R. Smith: "Analysis, Experimental results, and Range Adaptation of Magnetically Coupled Resonators for Wireless Power Transfer", *IEEE Trans. On Industrial Electronics*, Vol. 58, No. 2, pp. 544-554 (2011)

[12] S. Lee, R. D. Lorenz: "A Design Methodology for Multi-kW, Large Airgap, MHz Frequency, Wireless Power Transfer Systems", *IEEE ECCE 2011*, pp. 3503-3510 (2011)

[13] N. Hatti, Y. Kondo, H. Akagi: "Five-Level Diode-Clamped PWM Converters Connected Back-to-Back for Motor Drives", *IEEE Trans. On Industry Applications*, Vol. 44, No. 4, pp. 1268-1276 (2008)

[14] D. Ahn, S. Hong: "A Study on Magnetic Field Repeater in Wireless Power Transfer", *IEEE Trans. On Industrial Electronics*, Vol. 60, No. 1, pp. 360-371 (2013)

[15] T. Imura: "Equivalent Circuit for Repeater Antenna for Wireless Power Transfer via Magnetic Resonant Coupling Considering Signed Coupling", *6th IEEE Conf. On Industrial Electronics and Applications 2011*, pp. 1501-1506 (2011)

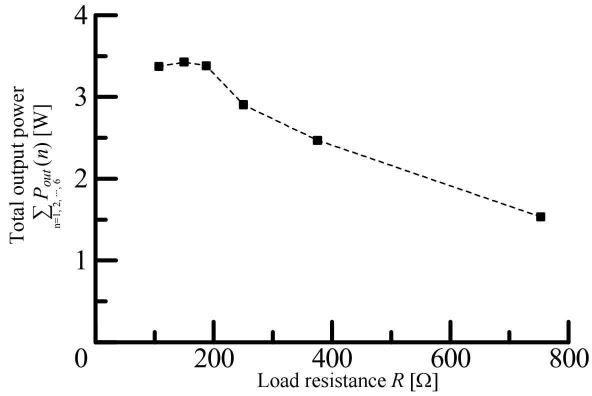

Fig. 17. Output power vs. load resistance. Owing to the voltage drop of the equivalent series resistance of the coils, the total output power is constrained at approximately 3.5 W.

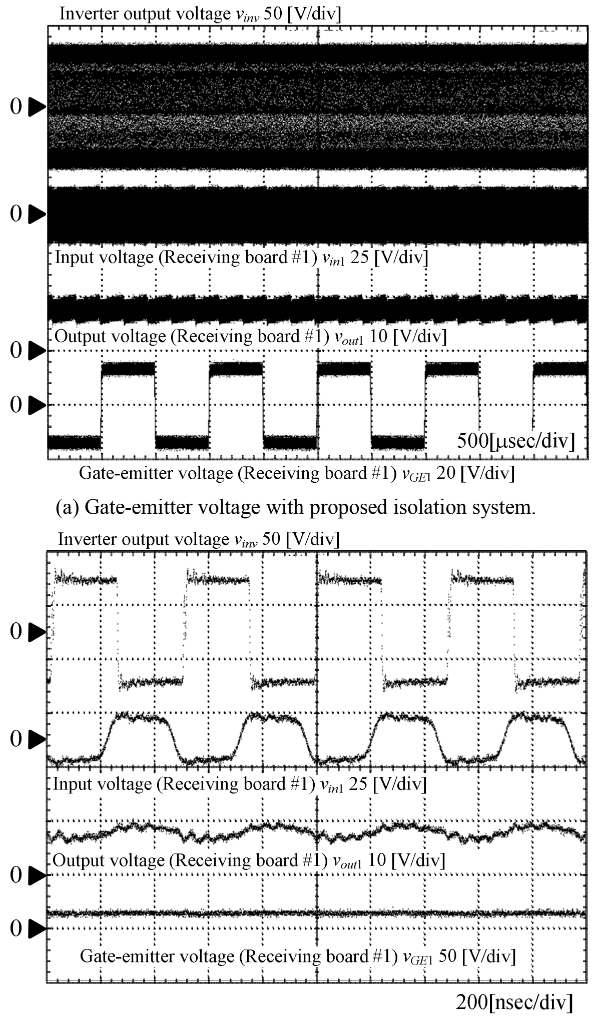

(a) Gate-emitter voltage with proposed isolation system.

(b) Extended operation waveforms of (a).

Fig. 18. Operation waveforms of the proposed isolation system with the gate drivers.